

or

$$\theta_0 \sim (l_0 U_1)^{-1},$$

$$\theta_0 \sim x^{1/2(m-1)}, \tag{28}$$

Thus the temperature length scale is proportional to the velocity length scale $l_0(x)$, and $\theta_0 \sim (u_0 U_1)$.

The lower and upper limits of m correspond to $\theta_0 \sim x^{-2/3}$ and $\theta_0 \sim x^{-1/2}$, respectively. This latter variation coincides with that which applies to a heated plane turbulent jet (e.g. Davies *et al.* [4]) for which $l_0(\sim l_0)$ varies approximately linearly. It should be noted that Townsend's conclusion [2] that the temperature scale must be proportional to the velocity scale ($\theta_0 \sim u_0$) is incorrect due to an erroneous statement of the conservation of momentum (for $|u_0| \ll U_1$).

For the case where $C_2 = C_3, U_1, u_0$ and l_0 admit exponential type solutions and it can be shown that

$$l_0 \sim e^{-3/2(\alpha_1 x)} \sim l_0, \tag{29}$$

$$\theta_0 \sim e^{1/2(\alpha_1 x)} \sim u_0 U_1. \tag{30}$$

Again, the conclusions of the previous paragraph remain valid for this case.

It is worthwhile to enquire whether the equation for the intensity of temperature fluctuation analogous to equation (9) is satisfied by the self-preserving distributions of $T, v\theta$ and

$$\left. \begin{aligned} \frac{1}{2} \overline{\theta^2} &= \theta_0^2 k_\theta(\eta), \\ \frac{1}{2} \overline{\theta^2 v} &= u_0 \theta_0^2 h_\theta(\eta), \\ v_\theta &= \frac{u_0 \theta_0^2}{l_0} e_\theta(\eta), \end{aligned} \right\} \tag{31}$$

Note that, since $l_0 \sim l_0$, no distinction is now made between ζ and η . The equation for $\theta^2/2$

$$U \frac{\partial}{\partial x} (\frac{1}{2} \overline{\theta^2}) + V \frac{\partial}{\partial y} (\frac{1}{2} \overline{\theta^2}) + v\theta \frac{\partial T}{\partial y} + \frac{\partial}{\partial y} (\frac{1}{2} \overline{\theta^2 v}) + e_\theta = 0$$

reduces to, neglecting terms of $O((u_0/U_1)^2)$,

$$2C_4 k_\theta - C_2 \eta k'_\theta + g_\theta f'_\theta + h'_\theta + e_\theta = 0. \tag{32}$$

Clearly, no new constraint emerges from (32) and the equation of the mean squared temperature fluctuation is satisfied by the assumed self-preserving forms in (31).

For an axisymmetric small-perturbation turbulent jet it is easy to show, using an approach analogous to that developed in [1] for the treatment of flow without heat transfer, that

$$\theta_0 \sim (U_1 l_0^2)^{-1} \sim u_0 U_1, \tag{33}$$

or

$$\theta_0 \sim x^{m-2/3}$$

since ([1])

$$l_0 \sim x^{1/3-m}$$

and $u_0 \sim x^{-2/3}$, irrespective of the value of m ($-\frac{2}{3} \leq m \leq -\frac{1}{3}$). There seems to be little if no experimental evidence available to support equations (28) or (33). The data obtained by Antonia and Bilger [5] in a heated round jet in a coflowing stream with no pressure gradient (the jet to external stream velocity ratio was 3) indicate that $\theta_0 \sim x^{-1}$ while (33) yields $\theta_0 \sim x^{-2/3}$. In this experiment, m is zero and therefore outside the range $-\frac{2}{3} \leq m \leq -\frac{1}{3}$ while the condition $|u_0| \ll U_1$ is not satisfied. At the last measurement station (the flow was still turbulent) $u_0 \approx 0.15 U_1$.

REFERENCES

1. I. S. Gartshore and B. G. Newman, Small perturbation jets and wakes which are approximately self-preserving in a pressure gradient, *CASI Trans.* **2**, 101-104 (1969).
2. A. A. Townsend, *The Structure of Turbulent Shear Flow*, Cambridge University Press, Cambridge (1976).
3. B. G. Newman, Turbulent jets and wakes in a pressure gradient, in *Fluid Mechanics of Internal Flow*, pp. 170-201, edited by G. Sovran. Elsevier, Amsterdam (1967).
4. A. E. Davies, J. F. Keffer and W. D. Baines, Spread of a heated plane turbulent jet, *Physics Fluids* **18**, 770-775 (1975).
5. R. A. Antonia and R. W. Bilger, The heated round jet in a coflowing stream, *AIAA J.* **14**, 1541-1547 (1976).

INFLUENCE OF TRANSVERSE INTRAPHASE VELOCITY PROFILES AND PHASE FRACTION DISTRIBUTIONS ON THE CHARACTER OF TWO-PHASE FLOW EQUATIONS

R. P. ROY and S. HO

Nuclear Engineering Program, University of Illinois, Urbana, IL 61801, U.S.A.

(Received 7 September 1979 and in revised form 21 January 1980)

NOMENCLATURE

a_{GL} , interfacial area per unit mixture volume;
 A_{x-s} , channel cross-sectional area;
 C_G, C_L, C_G^*, C_L^* , distribution coefficients (defined in text);
 \bar{f}_k , k -phase average of variable f
 $(\equiv \frac{1}{\Delta t_k} \int_{[\Delta t]_k} f_k dt)$;

F_{Bk} , body force on k -phase per unit mixture volume, z -component;
 F_{Wk} , frictional drag force on k -phase per unit mixture volume due to channel wall;
 \mathbf{g}_k , body force per unit mass of k -phase;
 j , $\sqrt{-1}$;
 p_k , k -phase static pressure;
 r , radial coordinate;

- \mathbf{r} , space vector;
- r^* , non-dimensional radial coordinate, r/R ($R =$ pipe radius);
- t , time;
- Δt , total time interval for Eulerian time-averaging;
- Δt_k , k -phase time interval;
- \mathbf{u}_k, u_{kz} , k -phase velocity vector, axial velocity;
- $\langle \bar{u}_{kz} \rangle_2, \langle \bar{u}_{kz} \rangle_3$, cross-sectional-average, volume-average axial velocities, k -phase;
- u_{Sk} , sonic velocity in k -phase;
- z , axial coordinate.

Greek symbols

- $\alpha_k, \langle \alpha_k \rangle_2, \langle \alpha_k \rangle_3$, local, cross-sectional-average, volume-average, k -phase fraction [$\alpha_k(\mathbf{r}, t) \equiv \Delta t_k(\mathbf{r}, t)/\Delta t$];
- γ_{GL} , coefficient for interfacial viscous drag term;
- ρ_k , density of k -phase;
- μ , coefficient for added mass term;
- η , coefficient for form drag term;
- π_k , viscous stress tensor, k -phase.

1. INTRODUCTION

A GREAT deal of attention has been focused in recent years on the character of two-phase (specially liquid–gas) flow conservation equations. Generally, the time- or ensemble-averaged and space-averaged transient one-dimensional form of the equations derived from the local, instantaneous equations (Delhaye and Achard [1], Ishii [2]) are of interest. These averaged forms are, however, often mathematically ill-posed as initial value problems (IVP) as indicated by the occurrence of complex characteristic roots (Gidaspow [3], Lyczkowski *et al.* [4]). Since the flow system under consideration represents a propagation problem, it can indeed be argued that the proper governing equation set should be non-elliptic [5] and therefore complex characteristic roots should not occur. Attempts to solve mixed hyperbolic–elliptic equation sets as initial value problems would lead to errors unless artificial stabilization is introduced into the solution scheme or computations are terminated prior to excessive error growth.

Addition of new terms and/or modification of existing terms, often on the basis of physical reasoning, have been suggested by various investigators in their efforts to render the governing equation sets well-posed as IVP. As examples, terms representing relative acceleration between the phases (Lyczkowski *et al.* [4]), inertial coupling between the phases (Soo [6], Chao *et al.* [7]), interfacial pressure forces (Stuhmiller [8]), unequal phase pressures (Banerjee *et al.* [9]), and surface tension effects (Ramshaw and Trapp [10]) have been considered. In this paper, we incorporate the transverse intraphase velocity profiles and transverse phase fraction distributions into the averaged form of the governing equations obtained by Eulerian time-averaging and volume-averaging of the local instantaneous equations and demonstrate their important influence on the character of the equation set. Introduction of intraphase transverse profiles of axial velocities and phase fraction distributions is really the incorporation, into the governing equations, of the sub-volume element-scale information that would otherwise be lost due to the space-averaging operation. Example cases of annular air–water flow based on works by Calvert and Williams [11] and Hewitt and Hall-Taylor [12], and of bubbly air–water flow based on studies by Delhaye and Galaup [13] and Sato and Sekoguchi [14] are adopted for demonstration.

† Δz is to be small relative to the pertinent length scales of transients of interest. It can be made infinitesimally small ($\Delta z \rightarrow 0$) since Eulerian time-averaging followed by cross-sectional-averaging would still enable consideration of interfacial pressure distribution effects [8].

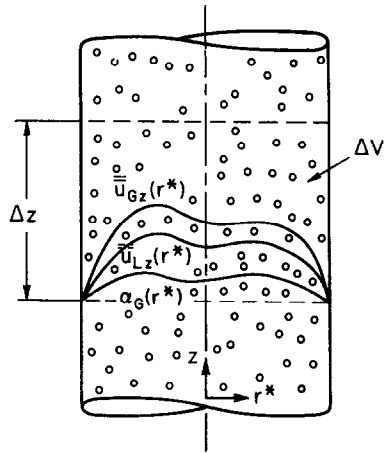


FIG. 1. Vertical upflow of gas–liquid bubbly mixture; transverse intraphase axial velocity profiles and local gas fraction distribution (schematic; $\Delta z \rightarrow 0$ allowed).

2. THE GOVERNING EQUATIONS

We consider adiabatic turbulent flow with no heat or mass transfer between the liquid and gas phase. A frame of reference fixed with respect to the flow channel is adopted. We begin with the local, instantaneous differential mass and linear momentum conservation equations for each phase ($k = G, L$):

$$\frac{\partial \rho_k}{\partial t}(\mathbf{r}, t) + \nabla \cdot [\mathbf{u}_k(\mathbf{r}, t)\rho_k(\mathbf{r}, t)] = 0 \tag{1}$$

$$\frac{\partial}{\partial t}[\rho_k(\mathbf{r}, t)\mathbf{u}_k(\mathbf{r}, t)] + \nabla \cdot [\mathbf{u}_k(\mathbf{r}, t)\rho_k(\mathbf{r}, t)\mathbf{u}_k(\mathbf{r}, t)] = \nabla \cdot [-p_k(\mathbf{r}, t)\mathbf{I} + \pi_k(\mathbf{r}, t)] + \rho_k \mathbf{g}_k \tag{2}$$

Let us consider vertical upflow in a pipe of constant cross-section. Performing the operations of Eulerian time-averaging [2] and averaging over a volume element $\Delta V (= A \times s \cdot \Delta z, \text{ Fig. 1})^\dagger$ fixed with respect to the frame of reference, equation (1) can be written, separately for two phases, per unit mixture volume as:

$$\frac{\partial}{\partial t}[\langle \alpha_G \rangle_3 \bar{\rho}_G] + \frac{\partial}{\partial z}[\langle \alpha_G \rangle_3 \bar{\rho}_G \langle \bar{u}_{Gz} \rangle_3 C_G^*] = 0 \tag{3}$$

$$\frac{\partial}{\partial t}[\langle \alpha_L \rangle_3 \bar{\rho}_L] + \frac{\partial}{\partial z}[\langle \alpha_L \rangle_3 \bar{\rho}_L \langle \bar{u}_{Lz} \rangle_3 C_L^*] = 0 \tag{4}$$

The axial (z) component of equation (2) can be written for the two phases, per unit mixture volume, as (with the aid of interfacial momentum jump condition):

$$\begin{aligned} & \frac{\partial}{\partial t}[\langle \alpha_G \rangle_3 \bar{\rho}_G \langle \bar{u}_{Gz} \rangle_3 C_G^*] + \frac{\partial}{\partial z}[\langle \alpha_G \rangle_3 \bar{\rho}_G \langle \bar{u}_{Gz} \rangle_3^2 C_G] \\ &= -\langle \alpha_G \rangle_3 \frac{\partial \bar{\rho}_G}{\partial z} + F_{WG} + F_{BG} - a_{GL}\gamma_{GL}[\langle \bar{u}_{Gz} \rangle_3 \\ & \quad - \langle \bar{u}_{Lz} \rangle_3] \pm \eta a_{GL}\bar{\rho}_L[\langle \bar{u}_{Gz} \rangle_3 - \langle \bar{u}_{Lz} \rangle_3]^2 \\ & \quad - \mu \bar{\rho}_L \langle \alpha_G \rangle_3 \left[\frac{\partial}{\partial t} \{ \langle \bar{u}_{Gz} \rangle_3 - \langle \bar{u}_{Lz} \rangle_3 \} \right. \\ & \quad \left. + \langle \bar{u}_{Gz} \rangle_3 \frac{\partial}{\partial z} \{ \langle \bar{u}_{Gz} \rangle_3 - \langle \bar{u}_{Lz} \rangle_3 \} \right] \end{aligned} \tag{5}$$

$$\begin{aligned} & \frac{\partial}{\partial t}[\langle \alpha_L \rangle_3 \bar{\rho}_L \langle \bar{u}_{Lz} \rangle_3 C_L^*] + \frac{\partial}{\partial z}[\langle \alpha_L \rangle_3 \bar{\rho}_L \langle \bar{u}_{Lz} \rangle_3^2 C_L] \\ &= -\langle \alpha_L \rangle_3 \frac{\partial \bar{\rho}_L}{\partial z} + F_{WL} + F_{BL} + a_{GL}\gamma_{GL}[\langle \bar{u}_{Gz} \rangle_3 \\ & \quad - \langle \bar{u}_{Lz} \rangle_3] \mp \eta a_{GL}\bar{\rho}_L[\langle \bar{u}_{Gz} \rangle_3 - \langle \bar{u}_{Lz} \rangle_3]^2 \end{aligned}$$

$$\begin{aligned}
 & + \mu \bar{\rho}_L \langle \alpha_G \rangle_3 \left[\frac{\partial}{\partial t} \{ \langle \bar{u}_{Gz} \rangle_3 - \langle \bar{u}_{Lz} \rangle_3 \} \right. \\
 & \left. + \langle \bar{u}_{Gz} \rangle_3 \frac{\partial}{\partial z} \{ \langle \bar{u}_{Gz} \rangle_3 - \langle \bar{u}_{Lz} \rangle_3 \} \right]. \tag{6}
 \end{aligned}$$

The coefficients η and μ depend on the prevalent flow structure (regime). The added mass term, derived on the basis of interfacial pressure distribution in [8], is somewhat similar in form to the inertial coupling term in [6, 7].

The θ -component of the momentum equation (2) is eliminated by assuming azimuthal symmetry. In the present work, we replace the r -component of the momentum equation by the assumption that the static pressure within each phase (excluding the interfaces) is uniform across the transverse (r)-dimension.

The distribution coefficients C_G and C_L appearing in equations (5) and (6) are[‡]:

$$\begin{aligned}
 C_G(z, t) &= \frac{1}{\Delta V} \int_{\Delta z} \int_{A_{X-S}} \alpha_g(r, t) \bar{u}_{Gz}^2(r, t) dA dz \\
 & \quad \frac{\langle \alpha_G \rangle_3(z, t) \langle \bar{u}_{Gz} \rangle_3^2(z, t)}{\langle \alpha_G \rangle_3(z, t) \langle \bar{u}_{Gz} \rangle_3^2(z, t)} \\
 & \cong \frac{1}{A_{X-S}} \int_{A_{X-S}} \alpha_g(r, z, t) \bar{u}_{Gz}^2(r, z, t) dA \\
 & \quad \frac{\langle \alpha_G \rangle_3(z, t) \langle \bar{u}_{Gz} \rangle_3^2(z, t)}{\langle \alpha_G \rangle_3(z, t) \langle \bar{u}_{Gz} \rangle_3^2(z, t)} \tag{7} \\
 C_L(z, t) &= \frac{1}{\Delta V} \int_{\Delta z} \int_{A_{X-S}} \alpha_l(r, t) \bar{u}_{Lz}^2(r, t) dA dz \\
 & \quad \frac{\langle \alpha_L \rangle_3(z, t) \langle \bar{u}_{Lz} \rangle_3^2(z, t)}{\langle \alpha_L \rangle_3(z, t) \langle \bar{u}_{Lz} \rangle_3^2(z, t)}
 \end{aligned}$$

We further assume that the axial pressure gradients are equal for the two phases:

$$\frac{\partial \bar{p}_G(z, t)}{\partial z} = \frac{\partial \bar{p}_L(z, t)}{\partial z} \tag{9}$$

Also:

$$\langle \alpha_G \rangle_3(z, t) + \langle \alpha_L \rangle_3(z, t) = 1. \tag{10}$$

3. CHARACTER OF THE EQUATIONS

The average conservation equations (3)–(6) can be written in the matrix form:

$$\mathbf{A} \frac{\partial \mathbf{U}}{\partial t} + \mathbf{B} \frac{\partial \mathbf{U}}{\partial z} = \mathbf{D} \tag{11}$$

where $\mathbf{U} = [\langle \bar{u}_G \rangle_3 \langle \bar{u}_L \rangle_3 \bar{p}_G \langle \alpha_G \rangle_3]^T$. The characteristic roots, λ , of equation (11) satisfy the relation:

$$\det |\mathbf{B} - \lambda \mathbf{A}| = 0. \tag{12}$$

To simplify the algebraic work, equation (5) is replaced by [equation (5) - $\langle \bar{u}_{Gz} \rangle_3 \cdot$ equation (3)], and equation (6) by [equation (6) - $\langle \bar{u}_{Lz} \rangle_3 \cdot$ equation (4)]. Sonic velocities in the gas and the liquid phases are introduced via the respective isothermal equations of state. Assuming, for simplicity, the distribution coefficients to be independent of z and t , equation (12), the characteristic equation, can then be written as:

$C_G^* \langle \alpha_G \rangle_3 \bar{p}_G$	0	$\frac{C_G^* \langle \alpha_G \rangle_3 \langle \bar{u}_{Gz} \rangle_3}{u_{SG}^2}$	$\bar{p}_G \langle \bar{u}_{Gz} \rangle_3 C_G^*$ $-\lambda \bar{p}_G$	= 0 (13)
0	$C_L^* \langle \alpha_L \rangle_3 \bar{p}_L$	$\frac{\lambda \langle \alpha_G \rangle_3}{u_{SG}^2}$	$\frac{C_L^* \langle \alpha_L \rangle_3 \langle \bar{u}_{Lz} \rangle_3}{u_{SL}^2}$ $-\bar{p}_L \langle \bar{u}_{Lz} \rangle_3 C_L^*$ $+ \lambda \bar{p}_L$	
$\langle \alpha_G \rangle_3 \bar{p}_G \langle \bar{u}_{Gz} \rangle_3 (2C_G - C_G^*)$ $+ \mu \bar{\rho}_L \langle \alpha_G \rangle_3 \langle \bar{u}_{Gz} \rangle_3$ $- \lambda [\langle \alpha_G \rangle_3 \bar{p}_G C_G^*]$ $+ \mu \bar{\rho}_L \langle \alpha_G \rangle_3$	$-\mu \bar{\rho}_L \langle \alpha_G \rangle_3 \langle \bar{u}_{Gz} \rangle_3$ $+ \lambda \mu \bar{\rho}_L \langle \alpha_G \rangle_3$	$\langle \alpha_G \rangle_3$ $+ \frac{(C_G - C_G^*) \langle \alpha_G \rangle_3 \langle \bar{u}_{Gz} \rangle_3^2}{u_{SG}^2}$ $\frac{\lambda \langle \alpha_G \rangle_3 \langle \bar{u}_{Gz} \rangle_3 (C_G^* - 1)}{u_{SG}^2}$	$\bar{p}_G \langle \bar{u}_{Gz} \rangle_3^2 (C_G - C_G^*)$	
$-\mu \bar{\rho}_L \langle \alpha_G \rangle_3 \langle \bar{u}_{Gz} \rangle_3$ $+ \lambda \mu \bar{\rho}_L \langle \alpha_G \rangle_3$	$\langle \alpha_L \rangle_3 \bar{p}_L \langle \bar{u}_{Lz} \rangle_3 (2C_L - C_L^*)$ $+ \mu \bar{\rho}_L \langle \alpha_G \rangle_3 \langle \bar{u}_{Gz} \rangle_3$ $- \lambda [\langle \alpha_L \rangle_3 \bar{p}_L C_L^*]$ $+ \mu \bar{\rho}_L \langle \alpha_G \rangle_3$	$\langle \alpha_L \rangle_3$ $+ \frac{(C_L - C_L^*) \langle \alpha_L \rangle_3 \langle \bar{u}_{Lz} \rangle_3^2}{u_{SL}^2}$ $\frac{\lambda \langle \alpha_L \rangle_3 \langle \bar{u}_{Lz} \rangle_3 (C_L^* - 1)}{u_{SL}^2}$	$-\bar{p}_L \langle \bar{u}_{Lz} \rangle_3^2 (C_L - C_L^*)$	

$$\cong \frac{1}{A_{X-S}} \int_{A_{X-S}} \alpha_l(r, z, t) \bar{u}_{Lz}^2(r, z, t) dA \tag{8}$$

Both C_G and C_L are usually equated to 1.0 in the literature, which is tantamount to assuming uniform velocity and phase fraction profiles. §

[‡] z represents the axial mid-plane of Δz in the event of a finite Δz .

§ $C_G^*(z, t)$ and $C_L^*(z, t)$ are similarly defined with \bar{u}_{Gz} and \bar{u}_{Lz} (instead of their squares) in the integrand of the numerators respectively.

Equation (13) is a quartic equation in λ and is simplified to a quadratic equation for the incompressible case ($u_{SG}, u_{SL} \rightarrow \infty$). The incompressible case equation is

$$\lambda^2 [\langle \alpha_L \rangle_3 C_G^* C_L^* (\langle \alpha_L \rangle_3 \bar{\rho}_G + \langle \alpha_G \rangle_3 \bar{\rho}_L) + \mu \bar{\rho}_L \langle \alpha_G \rangle_3 C_G^* + \langle \alpha_L \rangle_3 C_L^*] - \lambda [\langle \alpha_L \rangle_3^2 \bar{\rho}_G \langle \bar{u}_{Lz} \rangle_3 C_L^* (2C_G - C_L^*) + \langle \alpha_G \rangle_3 \langle \alpha_L \rangle_3 \bar{\rho}_L \langle \bar{u}_{Lz} \rangle_3 C_G^* (2C_L - C_L^*) + \langle \alpha_G \rangle_3 \langle \alpha_L \rangle_3 \bar{\rho}_L \langle \bar{u}_{Lz} \rangle_3 C_G^* C_L^* + \langle \alpha_L \rangle_3^2 \bar{\rho}_G \langle \bar{u}_{Gz} \rangle_3 C_G^* C_L^* + \mu \bar{\rho}_L \langle \alpha_G \rangle_3 \langle \bar{u}_{Lz} \rangle_3 C_G^* C_L^* + \langle \alpha_G \rangle_3 \langle \bar{u}_{Gz} \rangle_3 C_G^* + \langle \alpha_L \rangle_3 \langle \bar{u}_{Gz} \rangle_3 C_G^* + \langle \alpha_L \rangle_3 \langle \bar{u}_{Gz} \rangle_3 C_L^*] + C_G^* C_L^* [\langle \alpha_G \rangle_3 \langle \alpha_L \rangle_3 \bar{\rho}_L \langle \bar{u}_{Lz} \rangle_3^2 C_L + \langle \alpha_L \rangle_3^2 \bar{\rho}_G \langle \bar{u}_{Gz} \rangle_3^2 C_G + \mu \bar{\rho}_L \langle \bar{u}_{Gz} \rangle_3 \langle \alpha_G \rangle_3 \langle \bar{u}_{Lz} \rangle_3 + \langle \alpha_L \rangle_3 \langle \bar{u}_{Gz} \rangle_3] = 0 \tag{14}$$

Annular flow without entrainment

A range of flow conditions were studied in [11]. The following represents a particular air-water co-current vertical upflow case in a 28.4 mm dia. pipe:

$$\begin{aligned} \langle \bar{u}_{Gz} \rangle_3 &= 25.3 \text{ m s}^{-1}; & \langle \bar{u}_{Lz} \rangle_3 &= 0.631 \text{ m s}^{-1} \\ & \text{(corresponds to water film flow rate of } 90.72 \text{ kg h}^{-1}\text{);} \\ \langle \alpha_G \rangle_3 &= 0.9363; & \langle \alpha_L \rangle_3 &= 0.0637; \\ \text{temperature} &= 20^\circ\text{C}; & \text{system pressure} &= 1 \text{ atm.} \end{aligned}$$

The thermodynamic conditions yield:

$$\begin{aligned} \bar{\rho}_G &= 1.21 \text{ kg m}^{-3}; & \bar{\rho}_L &= 998 \text{ kg m}^{-3}; \\ u_{SG} &= 343.3 \text{ m s}^{-1}; & u_{SL} &= 1481 \text{ m s}^{-1}. \end{aligned}$$

We assume that a smooth interface exists between air and water. The transverse intraphase axial velocity profiles are approximated by (Fig. 2):

$$\begin{aligned} 0.0 \leq r^* \leq 0.9676; \\ \bar{u}_G(r^*), \text{ m s}^{-1} &= 375.2268 [(1 - r^*)^{1/5} + 0.2r^*] - 258.4564; \\ 0.9676 \leq r^* \leq 0.986; \\ \bar{u}_L(r^*), \text{ m s}^{-1} &= 12.035 - 7.1286r^* + 0.5928 \ln(1 - r^*) \\ & \text{(turbulent liquid region);} \\ 0.986 \leq r^* \leq 1.0; \\ \bar{u}_L(r^*), \text{ m s}^{-1} &= 176.7589 (1 - r^*) \text{ (viscous liquid layer).} \end{aligned}$$

The phase fraction profiles are flat across the respective regions in this case.

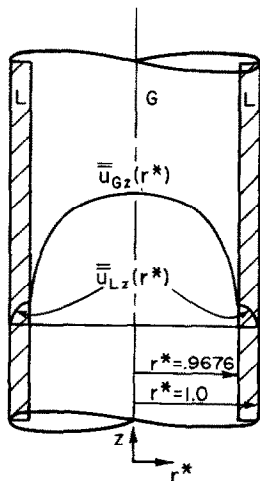


FIG. 2. Vertical turbulent upflow of air and water in annular configuration—smooth interface and no entrainment assumed.

Table 1(a)

(i) $C_L = 1.3796, C_G = 1.1158$		(ii) Flat transverse velocity profiles: $C_L = C_G = 1.0$	
(m s ⁻¹)		(m s ⁻¹)	
$\lambda_1 = -315.2066$	$\lambda_2 = 371.6615$	$\lambda_1 = -318.0157$	$\lambda_2 = 368.6116$
$\lambda_3 = 0.4813$	$\lambda_4 = 1.2643$	$\lambda_3 = 0.6331 - j0.2246$	$\lambda_4 = 0.6331 + j0.2246$

Table 1(b)

(i) $C_L = 1.3796, C_G = 1.1158$		(ii) Flat transverse velocity profiles: $C_L = C_G = 1.0$	
(m s ⁻¹)		(m s ⁻¹)	
$\lambda_1 = 0.4809$	$\lambda_2 = 1.2646$	$\lambda_1 = 0.6331 - j0.2241$	$\lambda_2 = 0.6331 + j0.2241$
The other two roots $\rightarrow \infty$		The other two roots $\rightarrow \infty$	

The distribution coefficients are calculated to be:

$$C_L = 1.3796, C_G = 1.1158; C_L^* = 1.0, C_G^* = 1.0;$$

μ is equal to 0.0. The characteristic roots for the case where compressibilities of the phases are taken into account are shown in Table 1(a). The characteristic roots for the incompressible case are shown in Table 1(b).

From the tables, it is clear that incorporation of the transverse intraphase velocity profiles has resulted in real characteristic roots in both the compressible and the incompressible cases. Especially noteworthy is the substantial inequality in the axial velocities of the two phases. If the transverse velocity profiles are not taken into account, then the only situation for which the characteristic roots would be real in the present example is equal phase velocities.

Bubbly flow

(a) A case based on measurements reported by Delhaye and Galaup [13] in air-water vertical upflow in a 42 mm I.D. pipe is considered:

$$\begin{aligned} \langle \bar{u}_{Gz} \rangle_3 &= 1.5921 \text{ m s}^{-1}; & \langle \bar{u}_{Lz} \rangle_3 &= 1.5863 \text{ m s}^{-1}; \\ \langle \alpha_G \rangle_3 &= 0.0544; & \langle \alpha_L \rangle_3 &= 0.9456; \\ \text{temperature} &= 20^\circ\text{C}; & \text{system pressure} &= 1 \text{ atm.} \end{aligned}$$

The thermodynamic conditions yield:

$$\begin{aligned} \bar{\rho}_G &= 1.21 \text{ kg m}^{-3}; & \bar{\rho}_L &= 998 \text{ kg m}^{-3} \\ u_{SG} &= 343.3 \text{ m s}^{-1}; & u_{SL} &= 1481 \text{ m s}^{-1}. \end{aligned}$$

The axial velocity and phase fraction profiles are approximated as:

$$\begin{aligned} 0.0 \leq r^* \leq 1.0; & \bar{u}_{Gz}(r^*) = 2.03 (1 - r^*)^{1/8}, \text{ m s}^{-1} \\ & \bar{u}_{Lz}(r^*) = 1.77 (1 - r^*)^{1/8}, \text{ m s}^{-1} \\ 0.0 \leq r^* \leq 0.50; & \alpha_G(r^*) = 0.0, \alpha_L(r^*) = 1.0 \\ 0.50 \leq r^* \leq 0.90; & \alpha_G(r^*) = 0.3995 (r^* - 0.50) \\ & \alpha_L(r^*) = (1.19975 - 0.3995 r^*) \\ 0.90 \leq r^* \leq 1.0; & \alpha_G(r^*) = 1.598 (1 - r^*) \\ & \alpha_L(r^*) = (1.598 r^* - 0.598). \end{aligned}$$

The distribution coefficients are calculated to be:

$$C_L = 0.8829, C_G = 1.2125; C_L^* = 0.9274, C_G^* = 1.1896.$$

Table 2(a)

μ	(i) $C_L = 0.8829, C_G = 1.2125$ $C_L^* = 0.9274, C_G^* = 1.1896$	(ii) Flat transverse velocity and phase fraction profiles: $C_L = C_G = C_L^* = C_G^* = 1.0$
	(m s ⁻¹)	
0.4	$\lambda_1, \lambda_2 = 1.6926 \pm j0.0831$	$\lambda_1, \lambda_2 = 1.5913 \pm j0.0013$
0.5	$1.699 \pm j0.0505$	$1.5914 \pm j0.0012$
0.6	1.7265, 1.6804	$1.5915 \pm j0.0012$
0.7	1.760, 1.6535	$1.5916 \pm j0.0011$
0.8	1.7772, 1.6413	$1.5916 \pm j0.0011$
1.0	1.7977, 1.6281	$1.5917 \pm j0.0008$

Table 2(b)

μ	(i) $C_L = 0.8829, C_G = 1.2125$ $C_L^* = 0.9274, C_G^* = 1.1896$	(ii) $C_L = C_G = C_L^* = C_G^* = 1.0$
	(m s ⁻¹)	
	$\lambda_1 = -54.1719$	-53.2877
	$\lambda_2 = 57.1555$	56.4615
	$\lambda_3 = 1.6804$	$1.5915 - j0.0015$
	$\lambda_4 = 1.7265$	$1.5915 + j0.0015$

Table 3

μ	(i) $C_L = 1.076, C_G = 1.007$ $C_L^* = 1.003, C_G^* = 0.990$	(ii) $C_L = 1.06, C_G = 1.06$ $C_L^* = 1.00, C_G^* = 1.00$	(iii) $C_L = C_G = 1.0$ $C_L^* = C_G^* = 1.0$
	(m s ⁻¹)		
0.1	$\lambda_1, \lambda_2 = 0.8411, 0.6617$	$\lambda_1, \lambda_2 = 0.8065, 0.6874$	$\lambda_1, \lambda_2 = 0.7241 \pm j0.1256$
0.2	0.8401, 0.7341	$0.7845 \pm j0.0293$	$0.7681 \pm j0.1268$
0.3	0.8695, 0.7446	$0.8056 \pm j0.0457$	$0.7928 \pm j0.1207$
0.4	0.8348, 0.8048	$0.8191 \pm j0.0491$	$0.8086 \pm j0.1138$
0.5	$0.8287 \pm j0.01$	$0.8285 \pm j0.0492$	$0.8196 \pm j0.1074$

Treating the added mass coefficient μ as a parameter, the characteristic roots for the incompressible case are as shown in Table 2(a). The two other roots $\rightarrow \infty$ in each of the above cases. The four characteristic roots for the compressible case, with $\mu = 0.6$, are as shown in Table 2(b). The roots for other μ -values are qualitatively similar to those in Table 2(a) (except of course that all four roots are finite now).

We observe that for Case (ii) the roots are imaginary for all values of μ , whereas for Case (i) where the transverse profiles have been incorporated they are real for $\mu \geq 0.6$. Since the shapes of flowing bubbles determine the value of the added mass coefficient (e.g. for end-on motion, $0 \leq \mu \leq 0.5$; for broad-side motion, $0.5 \leq \mu \leq 1.0$), a phenomenological explanation could be that the bubbles shapes here are such as to result in $\mu \geq 0.6$.

(b) We consider vertical upflow of isothermal air-water bubbly mixture in a 34.8 mm I.D. pipe, based on a study by Sato and Sekoguchi [14]:

$$\langle \bar{u}_{Gz} \rangle_3 = 0.9088 \text{ m s}^{-1}; \quad \langle \bar{u}_{Lz} \rangle_3 = 0.6218 \text{ m s}^{-1};$$

$$\langle \alpha_G \rangle_3 = 0.192; \quad \langle \alpha_L \rangle_3 = 0.808;$$

$$\text{temperature} = 13^\circ\text{C}; \quad \text{system pressure} = 1.38 \text{ bar};$$

$$\bar{\rho}_G = 1.682 \text{ kg m}^{-3}; \quad \bar{\rho}_L = 999.2 \text{ kg m}^{-3}.$$

The axial velocity and phase fraction profiles are approximated as:

$$0.0 \leq r^* \leq 0.91; \quad \bar{u}_G(r^*) = 0.9386 \text{ m s}^{-1},$$

$$\bar{u}_L(r^*) = 0.6915 \text{ m s}^{-1}$$

$$\alpha_G(r^*) = 0.2082,$$

$$\alpha_L(r^*) = 0.7918$$

$$0.91 \leq r^* \leq 1.0; \quad \bar{u}_G(r^*) = 10.4289(1 - r^*) \text{ m s}^{-1}$$

$$\bar{u}_L(r^*) = 7.6833(1 - r^*) \text{ m s}^{-1}$$

$$\alpha_G(r^*) = 2.3133(1 - r^*)$$

$$\alpha_L(r^*) = (2.3133r^* - 1.3133).$$

The distribution coefficients are calculated to be:

$$C_L = 1.076, C_G = 1.007; \quad C_L^* = 1.003, C_G^* = 0.990.$$

If only the transverse velocity profiles are taken into account but uniform phase fraction profile is assumed, then:

$$C_L = 1.06; \quad C_G = 1.06.$$

Results for the incompressible case are presented in Table 3 (the compressible case results are qualitatively similar).

We observe that for Case (iii) the roots are imaginary for all five values of μ , whereas for Case (ii) they are imaginary for four of the five values. For Case (i) where both velocity and phase fraction profiles have been included however, the roots are real for $\mu < 0.5$ (corresponds to end-on bubble motion).

Possible time-dependence of the various distribution coefficients raises further important questions unaddressed in this paper.

4. SUMMARY

Sub-volume element-scale information regarding transverse intraphase axial velocity profiles and phase fraction profiles were introduced into Eulerian time-averaged, volume-averaged (or cross-sectional-averaged) mass and axial momentum conservation equations thereby incorporating physical effects that would otherwise be lost as a result of space-averaging. It was shown that in case of models taking

phase compressibilities into account, governing equation sets which were mixed hyperbolic-elliptic originally could become strictly hyperbolic due to this improvement alone. In case of models assuming incompressibility, the same equation sets would become mixed hyperbolic-parabolic and thus still well-posed as a propagation problem. Optimum solution methods for such initial value problems can then be used with substantial benefits in regard to stability and accuracy.

REFERENCES

1. J. M. Delhaye and J. L. Achard, On the use of averaging operators in two-phase flow modeling, *Thermal and Hydraulic Aspects of Nuclear Safety*, Vol. 1, pp. 289-332. A.S.M.E., New York (1977).
2. M. Ishii, *Thermo-fluid Dynamic Theory of Two-phase Flow*. Eyrolles, Paris (1975).
3. D. Gidaspow, Modeling of two-phase flow, *Proceedings of the Fifth International Heat Transfer Conference*, Vol. VII, RT-1-2, p. 163. A.I.Ch.E., New York (1974).
4. R. W. Lyczkowski, D. Gidaspow, C. W. Solbrig and E. D. Hughes, Characteristics and stability analysis of transient one-dimensional two-phase flow equations and their finite-difference approximations, A.S.M.E. paper 75-WA/HT-23 (1975).
5. W. F. Ames, *Numerical Methods for Partial Differential Equations*. Barnes and Noble (1969).
6. S. L. Soo, On one-dimensional motion of a single component in two phases, *Int. J. Multiphase Flow* **3**, 79-82 (1976).
7. B. T. Chao, W. T. Sha and S. L. Soo, On inertial coupling in dynamic equations of components in a mixture, *Int. J. Multiphase Flow* **4**, 219-223 (1978).
8. J. H. Stuhmiller, The influence of interfacial pressure forces on the character of two-phase flow model equations, *Int. J. Multiphase Flow* **3**, 551-560 (1977).
9. S. Banerjee, R. L. Ferch, W. G. Mathers and B. H. McDonald, The dynamics of two-phase flow in a duct, *Proceedings of the Sixth International Heat Transfer Conference*, A.I.Ch.E., New York (1978).
10. J. D. Ramshaw and J. A. Trapp, Characteristics, stability, and short wavelength phenomena in two-phase flow equation systems, *Nucl. Sci. Engng* **66**, 93-102 (1978).
11. S. Calvert and B. Williams, Upward co-current annular flow of air and water in smooth tubes, *A.I.Ch.E. JI* **1**, 78-86 (1955).
12. G. F. Hewitt and N. S. Hall-Taylor, *Annular Two-phase Flow*. Pergamon Press, Oxford (1970).
13. J. M. Delhaye and J. L. Galaup, Hot-film anemometry in air-water flow, *Proceedings of the Fourth Symposium on Turbulence in Liquids*, University of Missouri-Rolla (1975).
14. Y. Sato and K. Sekoguchi, Liquid velocity distribution in two-phase bubble flow, *Int. J. Multiphase Flow* **2**, 79-95 (1975).